Supporting information for: An experimental study of clinopyroxene- and garnet-melt trace element partitioning in Fe-rich basaltic systems

M.D. Mouser[1,2,3] and N. Dygert[1]

[1]Department of Earth, Environmental & Planetary Sciences, University of Tennessee, Knoxville, TN, 37916, USA

[2]Earth and Planets Laboratory, Carnegie Institution for Science, Washington, D.C., 20015, USA

[3]Current Affiliation: Amentum, NASA Johnson Space Center, Astromaterials Research and Exploration Science, Houston, TX, 77058, USA

This file is supporting information for "An experimental study of clinopyroxene- and garnet-melt trace element partitioning in Fe-rich basaltic systems" by Mouser and Dygert. It contains figures referenced in the main text. Tables S1 and S2, which include major and trace element data on each experiment, can be found in the accompanying supporting information Excel file (Mouser, 2025) stored on Zenodo archive (https://doi.org/10.5281/zenodo.14721504). Below is a list of figures included in this file.

Figure S11. Pyroxene REE partition coefficients modeled using Al- and Fe-based M2 models from Dygert et al. (2014).

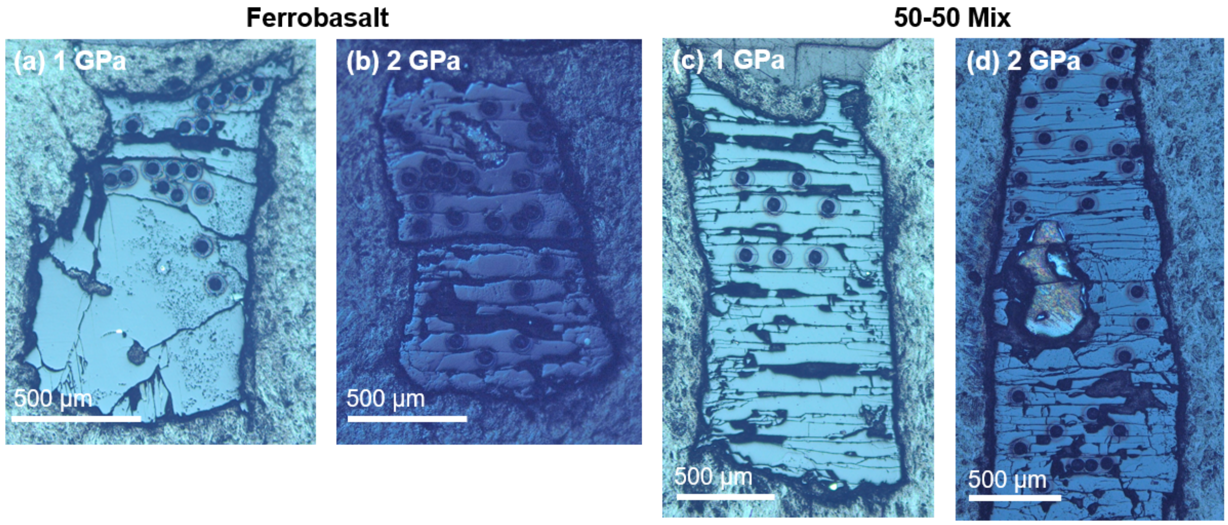

Figure S1. Reflected light images of experiments after LA-ICP-MS analysis of ferrobasalt (a,b) and 50-50 Mix (c,d) compositions at 1 and 2 GPa.

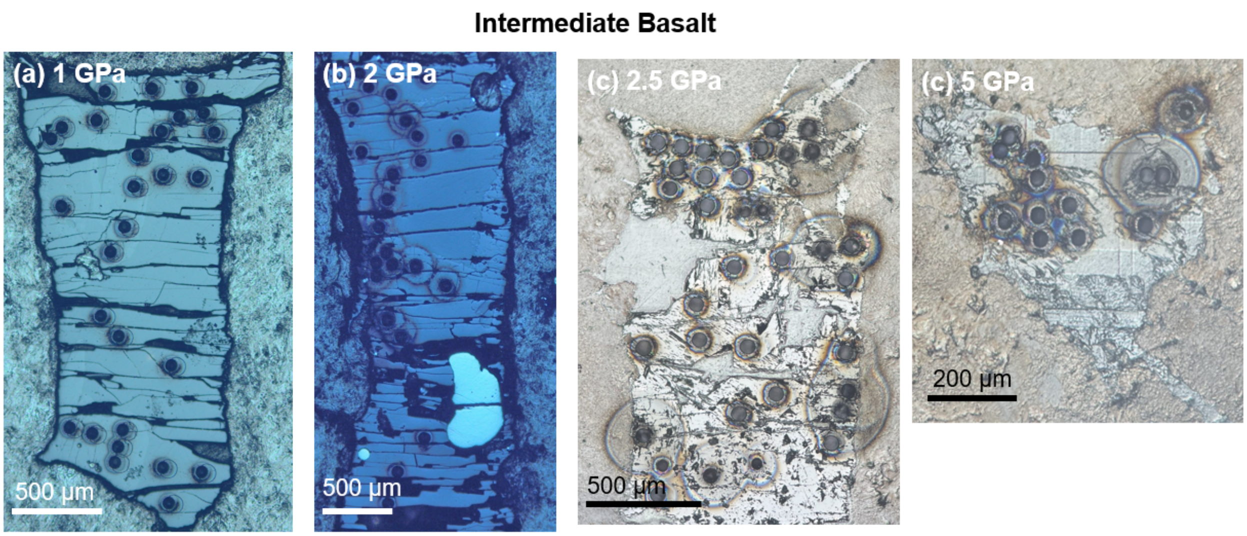

Figure S2. Reflected light images of intermediate basalt experiments after LA-ICP-MS analysis, (a) 1 GPa, (b) 2 GPa, (c) 2.5 GPa, and (d) 5 GPa.

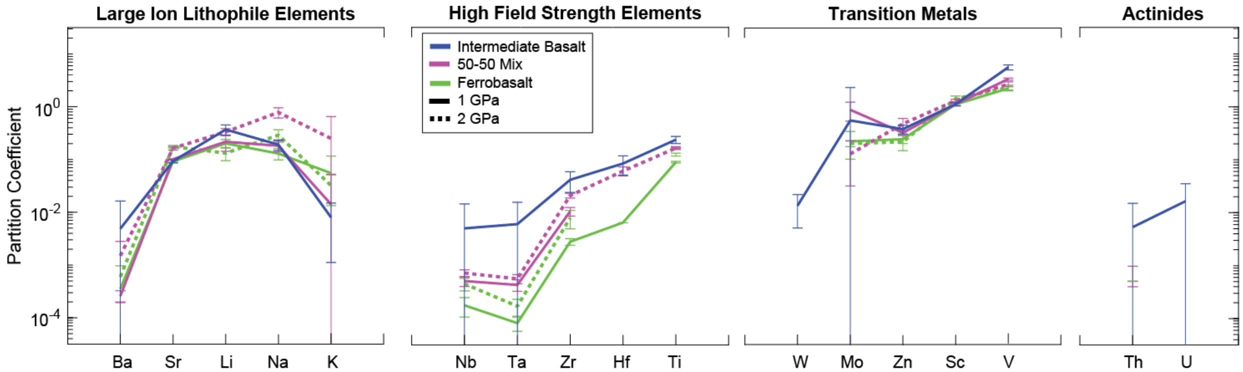

Figure S3. Pyroxene-melt partition coefficients for LILE, HFSE, transition metals, and U and Th calculated using Eq (1) from the pyroxene rim and glass data.

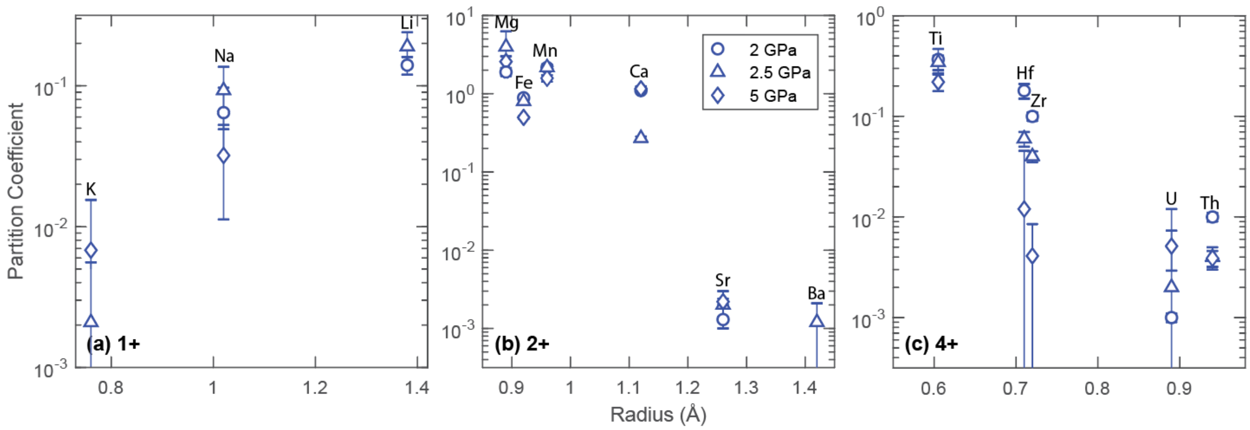

Figure S4. Garnet-melt partition coefficient for LILEs, HFSEs, and Actinides. Open symbols used for visual clarity.

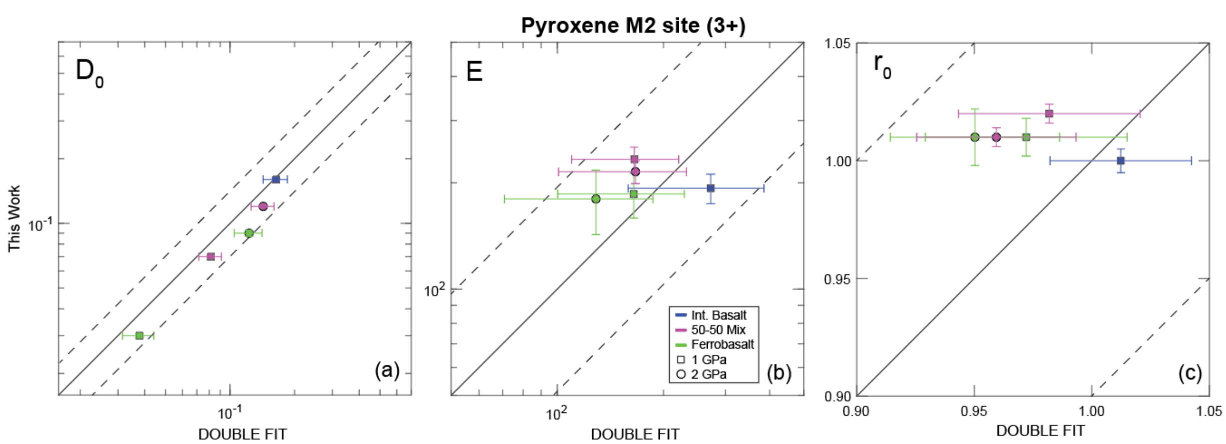

Figure S5. Lattice strain parameters for the M2 pyroxene site (3+) determined using DOUBLE FIT (Dalou et al., 2018) and the approach described in the main text (this work). The M2 site models are in good agreement. A direct comparison of trivalent element partition coefficient lattice strain parameters determined using DOUBLE FIT and the approach used in this study (see main text) for the M1 site could not be made due to the inclusion of V^{3+} in the calibrating data. Use of V repeatedly caused DOUBLE FIT to crash.

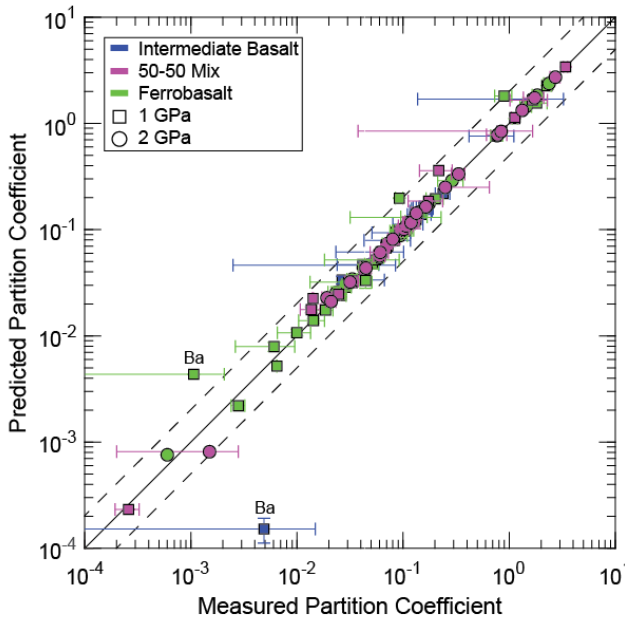

Figure S6. Measured vs predicted pyroxene partition coefficient values to demonstrate the quality of the lattice strain fits for each experiment.

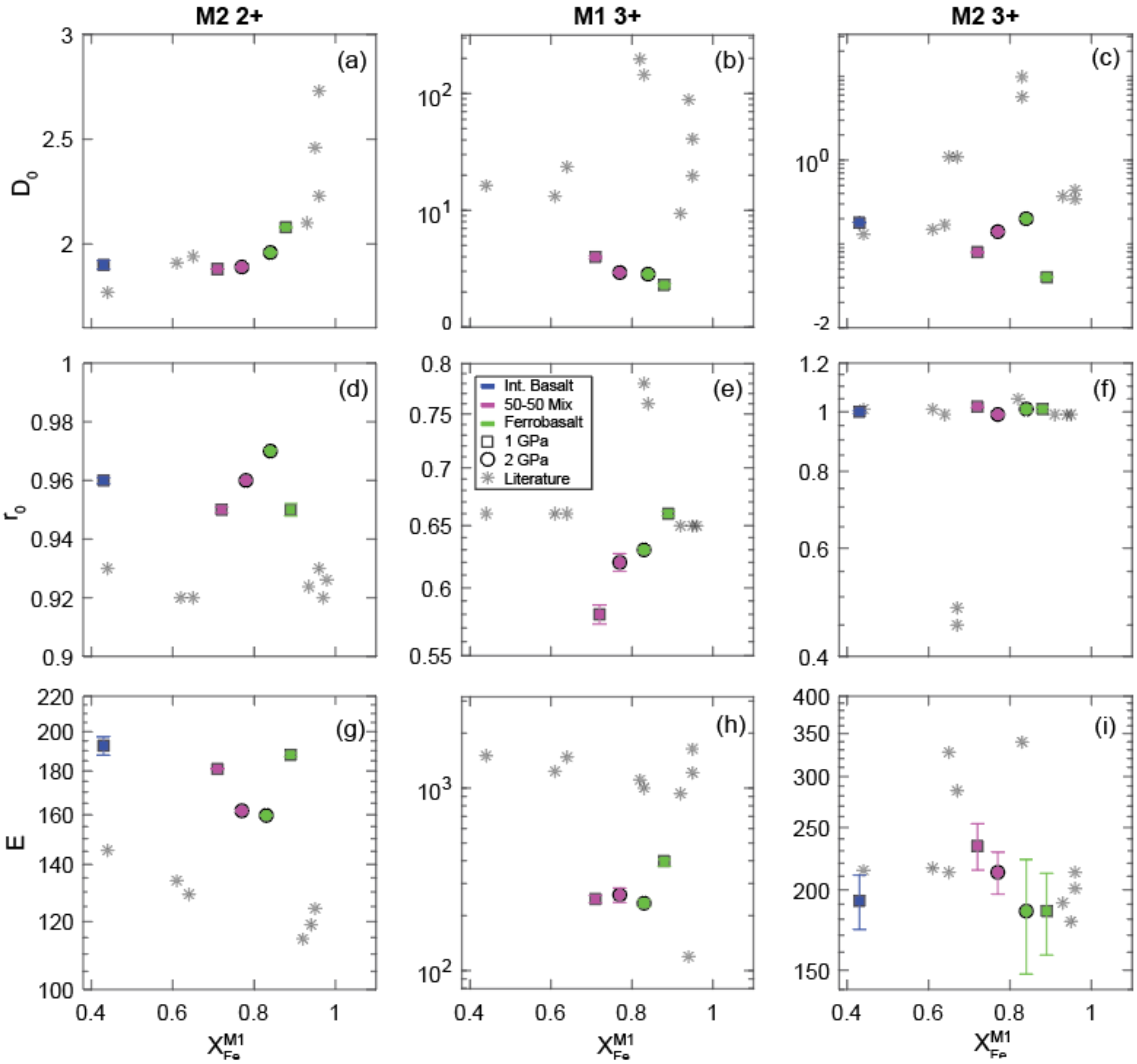

Figure S7. Lattice strain model parameters for pyroxenes produced in 1 and 2 GPa experiments plotted versus X_{Fe}^{M1}. Gray symbols indicate lattice strain model parameters from literature (Pertermann and Hirschmann, 2002; Olin and Wolff, 2010; Dygert et al., 2014).

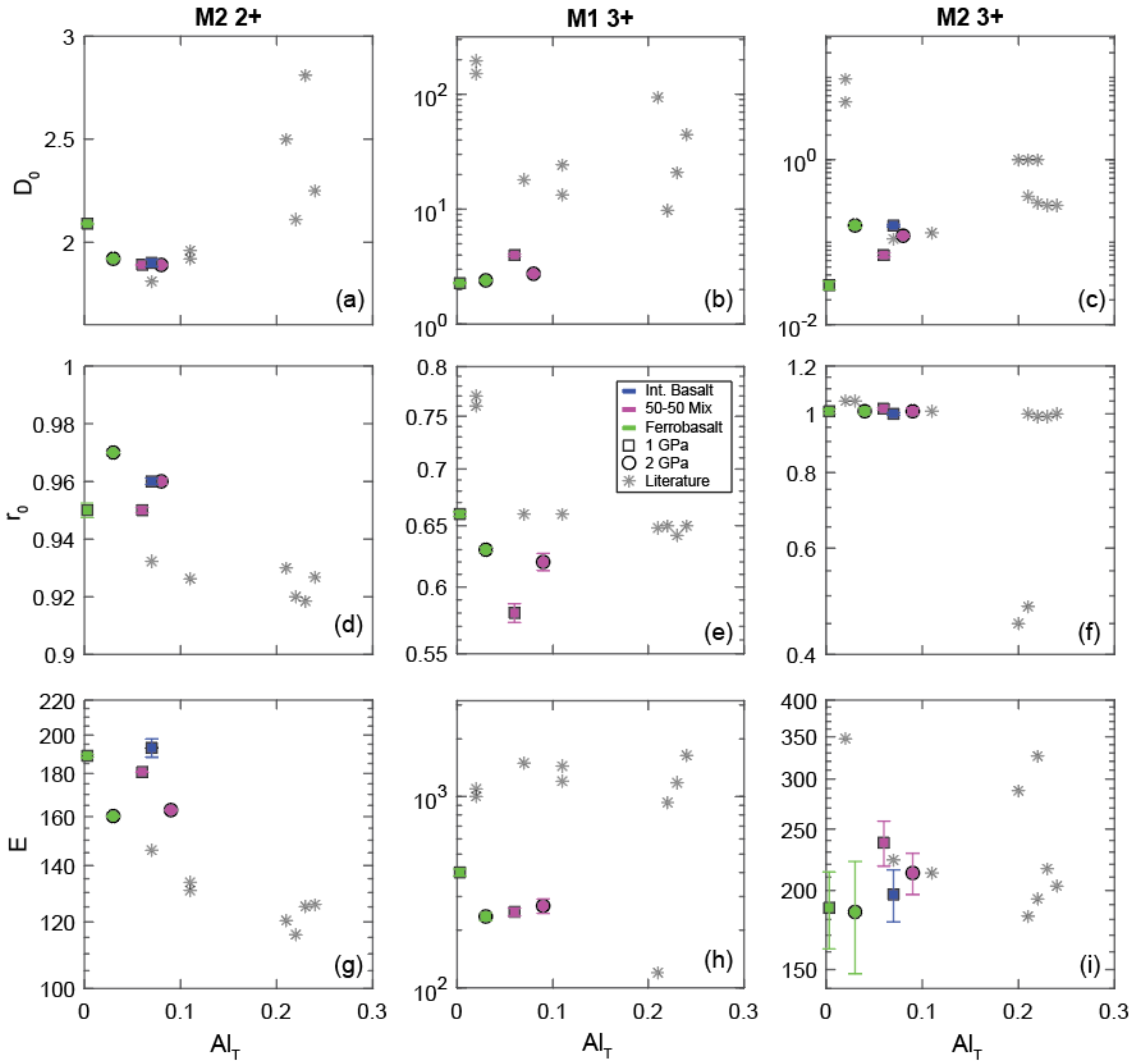

Figure S8. Lattice strain model parameters for pyroxenes produced in 1 and 2 GPa experiments plotted versus Al_T. Gray symbols indicate lattice strain model parameters from literature (Pertermann and Hirschmann, 2002; Olin and Wolff, 2010; Dygert et al., 2014).

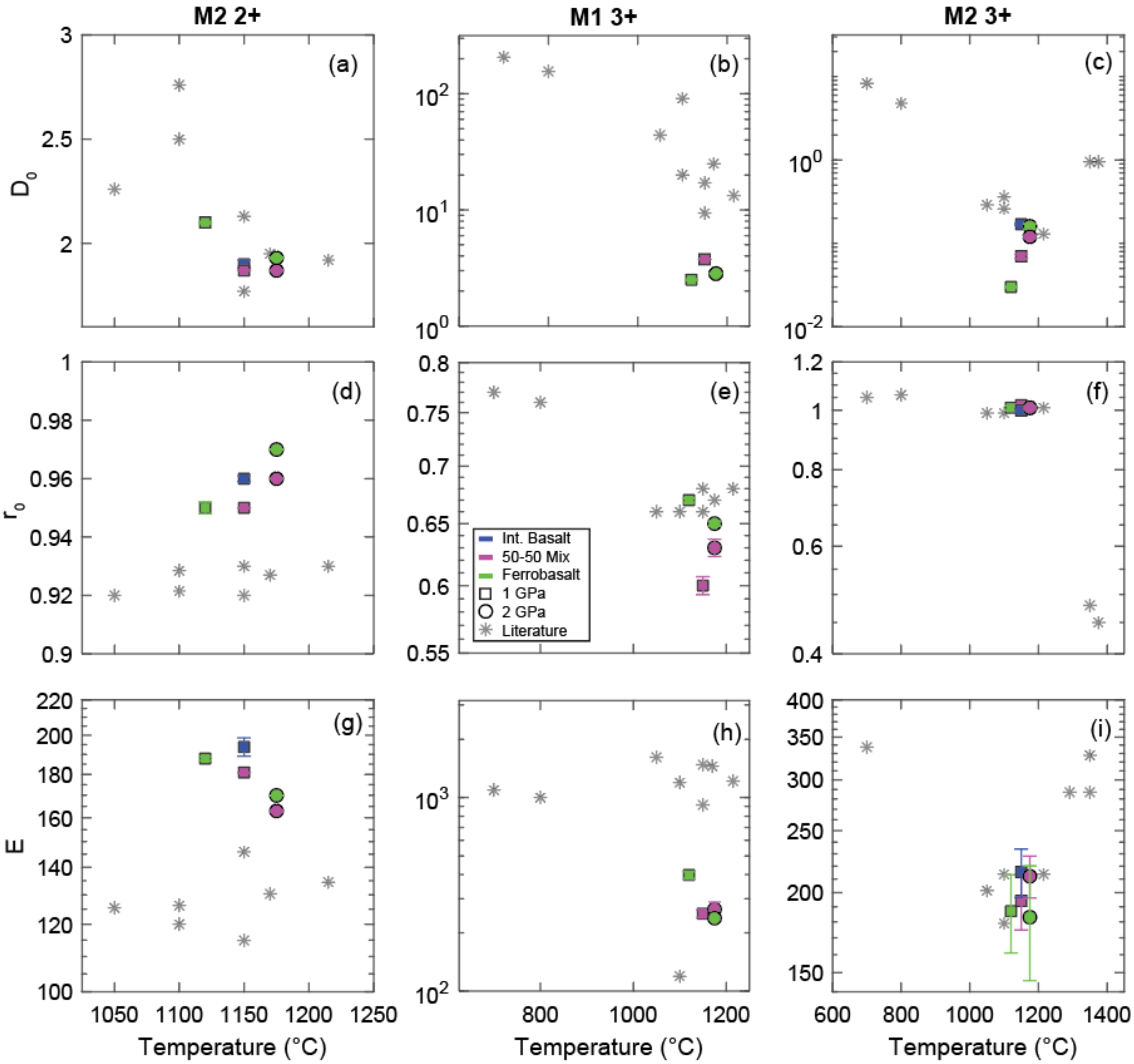

Figure S9. Lattice strain model parameters for pyroxenes produced in 1 and 2 GPa experiments plotted versus temperature. Gray symbols indicate lattice strain model parameters from literature (Pertermann and Hirschmann, 2002; Olin and Wolff, 2010; Dygert et al., 2014).

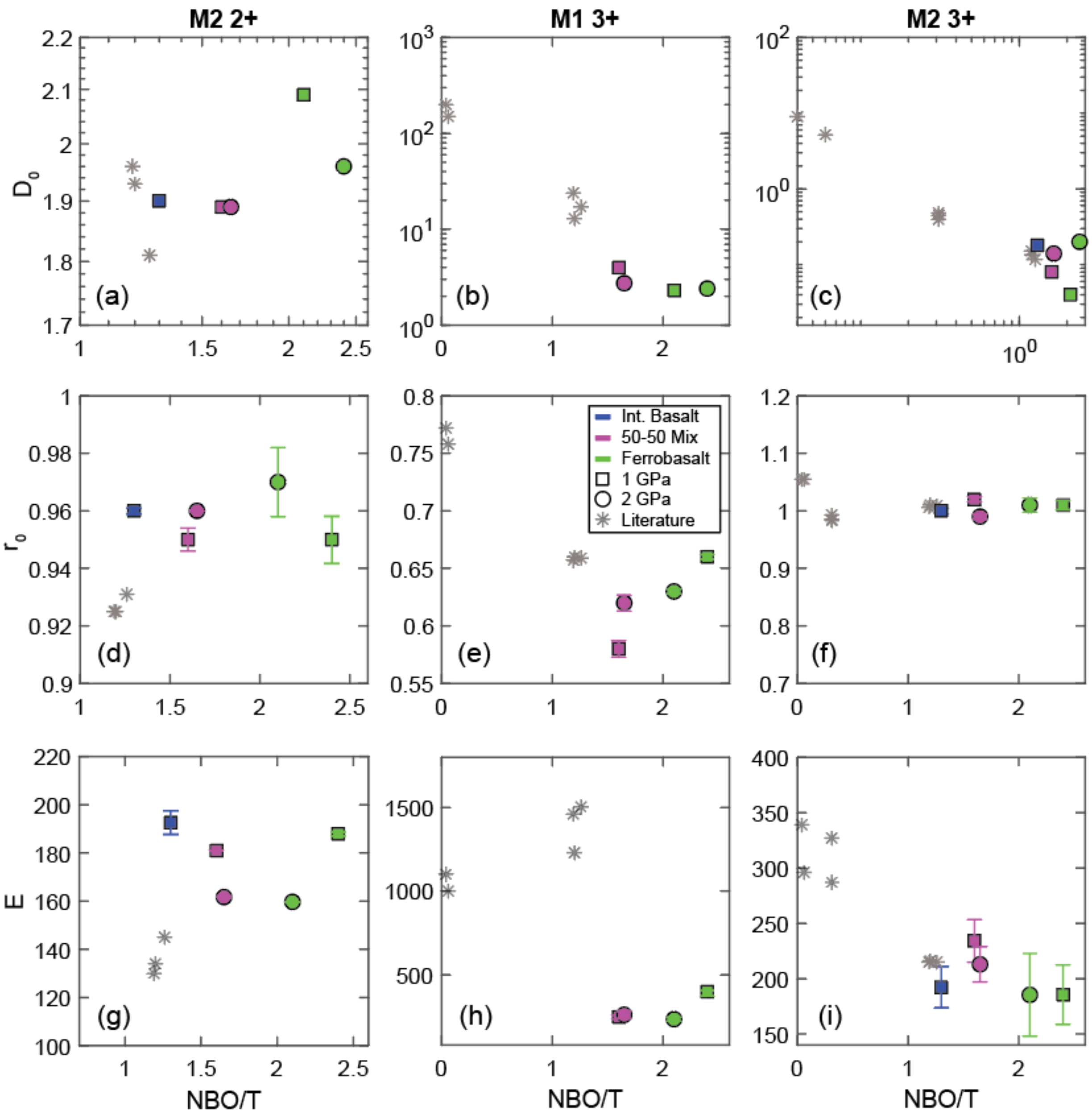

Figure S10. Lattice strain model parameters for pyroxenes produced in 1 and 2 GPa experiments plotted versus NBO/T. Gray symbols indicate lattice strain model parameters from literature (Pertermann and Hirschmann, 2002; Olin and Wolff, 2010; Dygert et al., 2014).

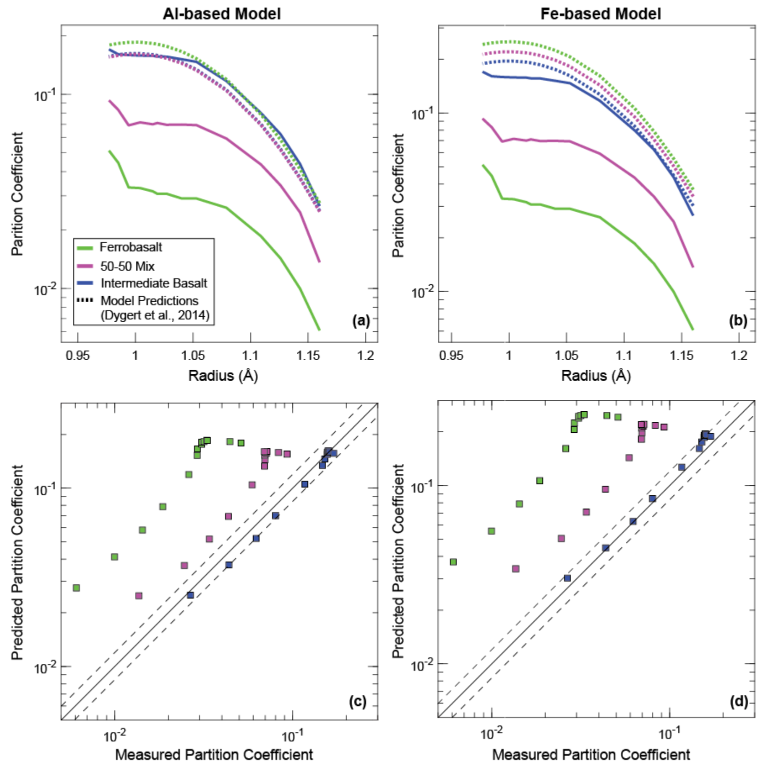

Figure S11. REE Al- and Fe-based model predictions from Dygert et al. (2014, 2015) for the three compositions and REE experimental measurements. (a-b) lattice strain parabolas, and (c-d) measured versus predicted partition coefficient. Note REEs are predicted assuming 8-fold coordination.

References

Dalou, C., Boulon, J., Koga, K. T., Dalou, R., Dennen, R. L. (2018). DOUBLE FIT: Optimization procedure applied to lattice strain model. *Computers and Geosciences, 117,* doi:10.1016/j.cageo.2018.04.013

Dygert, N., Liang, Y., Sun, C., & Hess, P. (2014) An experimental study of trace element partitioning between augite and Fe-rich basalts. *Geochimica et Cosmochimica Acta, 132,* 170-186. https://doi.org/10.1016/j.gca.2014.01.042

Dygert, N., Liang, Y., Sun, C., & Hess, P. (2015). Corrigendum to 'An experimental study of trace element partitioning between augite and Fe-rich basalts' [Geochim. Cosmochim. Acta 132 (2014) 170-186]. *Geochimica et Cosmochimica Acta* 149, 281-283. doi: https://doi.org/10.1016/j.gca.2014.01.042

Mouser, M. (2025). meganmouser/PxGt-Trace-Element-Partitioning: Updated files V1.2.2. https://doi.org/10.5281/zenodo.16056028

Olin, P. H. & Wolff, J. A. (2010) Rare earth and high field strength element partitioning between iron-rich clinopyroxenes and felsic liquids. *Contributions to Mineralogy and Petrology, 160,* 761-775. https://doi.org/10.1007/s00410-010-0506-2

Pertermann, M. & Hirschmann, M. (2002). Trace-element partitioning between vacancy-rich eclogitic clinopyroxene and silicate melt. *American Mineralogist, 87*, 1365-1376. https://doi.org/10.2138/am-2002-1012